AIAA 81-1896R

Development of Analytical and Experimental Techniques for Determining Store Airload Distributions

Charles H. Morgret* and Richard E. Dix†
Calspan Field Services, Inc., AEDC Division, Arnold Air Force Station, Tennessee
and
L.E. Lijewski‡
Air Force Armament Laboratory, Eglin Air Force Base, Florida

A semiempirical computer code has been developed for the prediction of the distribution of static aerodynamic loads acting on a store both in the free stream and in the interference flow field of an aircraft. The code is applicable to a wide range of configurations for subsonic through supersonic Mach numbers and angles of attack to approximately 45 deg. Wind tunnel tests were conducted using a 1/4-scale pressure model, a 1/4-scale force model divided into four segments, and a three-segment 1/20-scale force model of the same configuration. Integrated pressure data, segmented force data, and previously obtained single balance data agreed well, and computer code predictions correlated well with the experimental data.

Nomenclature

C_{D_c} = cross-flow drag coefficient = (viscous cross-flow force per unit length)/$g_\infty d\sin^2\alpha$
C_m = pitching-moment coefficient = (pitching moment)/$q_\infty dS$
C_N = normal-force coefficient = (normal force)/$q_\infty S$
C_{N_c} = coefficient of force acting in the cross-flow plane, = (cross-flow force)/$q_\infty S$
C_{N_f} = coefficient of force acting normal to a fin = (fin normal force)/$q_\infty S$
C_p = pressure coefficient, = (pressure minus free-stream static pressure)/q_∞
C_Y = side-force coefficient = (side force)/$q_\infty S$
$c.p.$ = longitudinal center of pressure
d = store maximum diameter, ft
L = store body length, in.
M = freestream Mach number
M_c = cross-flow Mach number
M_{local} = local Mach number
q_{local} = local dynamic pressure, lb/ft^2
q_∞ = free-stream dynamic pressure, lb/ft^2
S = store maximum cross-sectional area, ft^2
t = time, s
V_c = cross-flow velocity, ft/s
V_x = local velocity component along the store x axis, ft/s
V_y = local velocity component along the store y axis, ft/s
V_z = local velocity component along the store z axis, ft/s
V_∞ = free-stream velocity, ft/s
x = store axial coordinate, measured from the nose tip, positive rearward, ft
y = store lateral coordinate, positive to the left looking in the $+x$ direction, ft
z = store vertical coordinate, positive upward, ft
α = free-stream angle of attack, deg
α_f = fin angle of attack, deg
α_T = total local angle of attack = $\tan^{-1}(V_c/V_x)$, deg
η = correction to C_{D_c} for finite-length bodies
ϕ = roll orientation with respect to the z axis, positive counterclockwise looking in the $+x$ direction, deg

Presented as Paper 81-1896 at the AIAA Atmospheric Flight Mechanics Conference, Albuquerque, N. Mex.; Aug. 19-21, 1981. Submitted Sept. 30, 1981; revision received April 22, 1982.

*Research Engineer, 4T Projects Branch Propulsion Wind Tunnel Facility. Member AIAA.
†Senior Research Engineer, 4T Projects Branch, Propulsion Wind Tunnel Facility. Member AIAA.
‡Project Manager, Aircraft Stores Compatibility Branch. Member AIAA.

Introduction

AIRCRAFT combat effectiveness is highly dependent upon the ability to carry and deliver ordnance with minimum penalty to speed and maneuver performance. Operational performance can be severely penalized by aerodynamic drag, inadequate structural integrity, poor store separation trajectories, and stability and control problems. These problems can be significantly reduced by proper design of weapons and the development of accurate techniques for predicting the behavior of proposed aircraft/weapon configurations and store separation trajectories. Accurate and cost-effective store carriage and separation prediction techniques are needed to provide design criteria for weapon development programs, issue clearances for aircraft/store flight test programs, and conduct aircraft/store certification programs. Current methods to predict aerodynamic loadings on captive stores for structural integrity and store separation analyses are overconservative resulting in overdesigned, structurally inefficient stores. Classical pressure testing to obtain captive store aerodynamic loadings is prohibitively expensive when done for many configurations. To be cost-effective, the testing technique must be applicable to small-scale stores which permit testing in smaller, less expensive wind tunnels. An accurate prediction technique and cost-effective testing method are required to obtain captive store aerodynamic loading distributions.

To establish the capability of obtaining airloads distributed over captive stores, a four-year analytical and experimental development program was begun in 1979. The effort consists of formulating a computer program prediction code concurrently with the development of valid wind tunnel testing

techniques. In developing the prediction code, the Aerodynamic Coefficients Module of the Computer Aided Missile Synthesis (CAMS) Program[1] was selected as a starting point. This semiempirical code was chosen because it had the inherent capability of calculating distributed aerodynamic loadings on stores in the free-stream. The capability to calculate the distributed airloads over a captive store resulted when the code was modified to accept an interference flow-field by allowing the angle of attack to vary along the store.

Validation of this prediction code with wind tunnel data required the development of a unique testing technique. A sound base on which to build the new test technique was established using a classical pressure test of a 1/4-scale store in the free-stream. A force and moment test was then conducted on a store of the same scale segmented into four sections, each with a separate balance. Results from the segmented force test were compared to forces obtained from integration of the pressure test data to validate the segmented technique. In addition, to assure that the segmented store technique could be valid at a small scale, a 1/20-scale free-stream force and moment test of the same store was completed and results compared to the larger scale data. Data from these tests were then compared to results from the prediction code to determine the accuracy of the prediction model. Currently, the interference flow-field version of the prediction code is nearing completion. A 1/20-scale segmented store was tested in the carriage position late in FY81. The store was segmented into three sections to obtain force and moment data along the store. These data are being used for validation of the interference prediction code.

Development of the Prediction Technique

The Aerodynamic Coefficients Module of the CAMS program was selected as the starting point for developing a prediction technique because it contained an option permitting the calculation of distributed loads for a wide range of store configurations and flight conditions. Configuration options include various nose shapes, cone or ogive boattail, and one or two sets of fins. Fin options include single- or double-delta planforms, several circumferential arrangements, and various symmetrical airfoil sections. A cylindrical centerbody is required, and one set of fins must be designed as all-movable control surfaces. Angle of attack (α) may range from 0 up to 10 deg beyond fin stall, and Mach numbers (M) from 0.5 to 10.0 are permitted. For the distributed loads calculation, the nose of the store is divided into eight segments, the centerbody is treated as one segment, and the boattail (if present) is divided into three segments. Normal- and axial-force coefficients are calculated for each segment. Force coefficients for each set of fins are calculated separately, with fin-alone coefficients modified to account for vortex effects and body upwash. Loads on the body attributable to the fins are calculated independently of body-alone loads.

A preliminary prediction code known as the Distributed Loads (DL) code was formed by extracting from CAMS those sections required to calculate load distributions in the range of interest. In order to provide the desired interference flow-field capability, the DL code was modified to allow varying flow conditions along a store. Methodology was improved in areas where the code was known to be weak and where comparison with experimental data showed major discrepancies. Areas for possible further development have been identified.

Free-Stream Code Development

The DL code was extracted from the CAMS aerodynamic coefficients module by deleting those sections of the module pertaining to configuration options for which the distributed loads calculation was not made (e.g., inlet and engine options), those calculations not relevant to the distributed loads calculation (e.g., tail sizing routines, C_m vs C_N tables), and those sections pertaining to flight regimes ($\alpha > 90$ deg or $M > 4$) outside the range of intended DL code application. This was done to reduce computer storage space and run time requirements (references to computer requirements pertain to the IBM 370/165 FORTRAN IV-G compiler) and to provide a smaller, simpler program that could be modified without concern for effects on the complex structure of CAMS. Numerous errors and inconsistencies were revealed in the original CAMS code through a detailed study of the distributed loads calculation, as a result of the extraction process and in attempting to match DL code results to those obtained using the CAMS distributed loads option. Most of the errors were programming errors, simple oversights or invalid extensions of small-angle approximations to large angles. The errors were corrected in the DL code. The DL code was then restructured to further reduce computer requirements.

The above changes resulted in a reduction of approximately 70% in required storage space and a substantial reduction in run time as compared to the original CAMS distributed loads option. The corresponding reductions in length and level of complexity also made the DL code much easier to work with than the CAMS program, facilitating further development.

Interference Code Development

Extensive modification of the DL code to permit calculations in an interference flowfield resulted in the Interference Distributed Loads (IDL) code. Free-stream capability was retained in the IDL code to avoid the need to apply subscequent methodology improvements to two separate programs and because some modifications necessary for calculations in an interference flow-field also had the potential to improve free-stream predictions.

Variations in flow conditions along the store were accounted for by using local rather than free-stream conditions to calculate loads on each body segment and each fin. The number of body segments was made variable with a maximum of 50. Because the free-stream code calculated only pitch-plane loads, the capability to compute side-force coefficients had to be added. The coefficient of force acting on a body segment in the cross-flow (y-z) plane (C_{N_c}) is determined using the total local angle of attack (α_T), then resolved into y and z components (see Fig. 1). Fin normal-force coefficients (C_{N_f}) are calculated individually, with fin angle of attack (α_f) determined by the component of V_c normal to the fin surface, and resolved into store-axis y and z components. The carryover load on the body attributable to a set of fins is determined based on the total load on that set of fins. All coefficients are referenced to the maximum body cross-sectional area (S) and to free-stream dynamic pressure (q_∞). Force coefficients for the total configuration are obtained by summing the individual contributions. Total pitching- and yawing-moment coefficients are determined similarly, using predicted fin centers of pressure and assuming that the load on a body segment acts at the center of the segment.

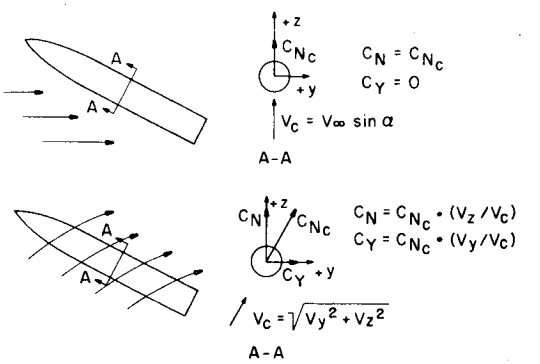

Fig. 1 Resolution of body-alone loads in the IDL code.

Flow parameters in the interference flow-field required to define local conditions for IDL code calculations were identified as V_y/V_x, V_z/V_x, M_{local}, and $q_{\text{local}}/q_\infty$. The code was modified to obtain values of these parameters by linear interpolation of input flow-field data in a two-step process. An initial interpolation in M and α provides a complete flow-field grid at input free-stream conditions. Thereafter, interpolation in x, y, and z within the grid provides values of the above parameters at desired locations along a store. Local flow conditions for a body segment were assumed to be those at the center of the segment. For a fin, as a simple initial assumption, the conditions at the midpoint of the leading edge were used.

Initial assumptions regarding the effects of a variable flow-field on vortex behavior were required. Body vortices were assumed to remain symmetric about the local cross-flow velocity vector (V_c). An iterative procedure was added to the code to determine the body vortex separation point. The separation point is first predicted based on the total angle of attack at the nose tip; thereafter, the prediction is refined based on the total angle of attack at the last predicted separation point. Body vortex height and lateral spacing are predicted by dividing the vortex path into a number of longitudinal points, and using the vortex position and total angle of attack (at the body centerline) at each point to determine the position at the next point. Wing vortices are tracked individually in a similar manner; however, the local conditions at each predicted vortex location are used rather than the conditions at the body centerline.

Methodology Modifications

During the development of the IDL code, original CAMS methods in need of improvement were addressed. Major modifications were made to body cross-flow drag calculations, application of fin interference factors, and prediction of fin center-of-pressure variation with angle of attack.

The original method for calculating the viscous contribution to the normal force on a body segment assumed a constant value of the cross-flow drag term ηC_{D_c} along the body. Because C_{D_c} was calculated as a function of cross-flow Mach number (M_c), it was necessary to introduce a variation along the body because of local M_c variations in an interference flow-field. To better represent the body normal-force distribution both in the free-stream and in an interference flow-field, the local variation of ηC_{D_c} attributable to other effects was also modeled. The correction factor for finite body length (η) was replaced with a local correction factor (adapted from Ref. 2) based on distance from an end of the body. Because the original method was limited to turbulent flow, the two-dimensional C_{D_c} calculation was modified to include local Reynolds number effects, thus allowing laminar, transitional, and turbulent flow. The local Reynolds number was assumed, as in Ref. 2, to be the vector sum of the axial- and cross-flow Reynolds numbers. The two-dimensional C_{D_c} curves used were taken from Refs. 3 and 4. A method for calculating the transient variation of C_{D_c} along the body was derived from Refs. 2 and 5. It was assumed, based on data presented in Ref. 6, that the transient effect disappears in turbulent flow. [The transient variation of C_{D_c} is based on the observation that, in laminar flow, the variation of C_{D_c} with x along a cylindrical body at angle of attack (α) is analogous to the variation of C_{D_c} with time on an infinite-length cylinder impulsively accelerated from rest to a velocity V_c, as shown in Fig. 2.] An empirical correction for axial pressure gradients on the nose and boattail was taken from Ref. 5.

The prediction of carryover and vortex interference effects on fin-alone normal force at high angles of attack was substantially improved by adopting an "equivalent angle-of-attack" method, described in Ref. 7. The original method of applying interference factors was derived in Ref. 8 for small angles of attack, using the approximation $\tan \alpha_f = \alpha_f$ and assuming fin C_{N_f} linear with α_f. The modified method uses essentially the same interference factors but applies them in a manner more valid for high angles of attack. The original method predicted C_{N_f} using fin-alone angle of attack. The interference factors were then applied to the fin-alone C_{N_f} to obtain C_{N_f} of the fin installed on the body. The modified method applies the interference factors to the tangent of the fin-alone angle of attack to obtain an equivalent angle of attack. The equivalent angle of attack is then used to predict C_{N_f} of the installed fin directly. A correction to carryover interference factors as a function of M and α was adopted from an updated version of CAMS.[9] The modification of the code to permit separate calculations for each fin, which was necessary for interference flow-field modeling, resulted in a better representation of vortex effects on X-cruciform fin arrangements in the free-stream as well. The original method did not account for the difference in vortex effects between the upper and lower fins of an X-cruciform arrangement.

The original method for predicting fin longitudinal center-of-pressure (c.p.) assumed no variation with fin angle of attack. A correction for nonzero angles of attack is mentioned in the CAMS literature[1] but did not appear in the CAMS program. A method for predicting the variation of fin c.p. location with angle of attack was derived from the DATCOM[10] and MISSILE[7] programs. The original methods for predicting c.p. at $\alpha_f = 0$ and for predicting fin stall angle were retained. Fin c.p. at the stall angle is predicted using a DATCOM method up to $M = 0.6$, the MISSILE method above $M = 0.8$, and fairing the two methods between $M = 0.6$ and 0.8. Corrections for leading-edge sharpness and nonzero trailing-edge sweep used in the DATCOM method were added to the MISSILE method. DATCOM methods are used to predict c.p. variation with angle of attack up to $M = 1.0$ as a function of c.p. at $\alpha_f = 0$, c.p. at the stall angle and fin geometry. For $M > 1.0$, it was assumed that c.p. varied linearly between the $\alpha_f = 0$ value and the value at the stall angle and linearly from the value at the stall angle to the fin's area centroid at a 90-deg angle of attack. The original CAMS method for predicting the c.p. of the body carryover load attributable to the fins was retained for $\alpha = 0$. At nonzero angle of attack, the body carryover c.p. was assumed to move the same distance and direction as the fin c.p. Refinements to the methods for predicting both the magnitude and the c.p. of body carryover loads are being studied.

A number of improvements to vortex calculations are also being studied. The current methods used for computing body vortex separation point, strength, and tracking are based on limited data and generally overpredict body vortex strength. The assumptions currently used for wing vortex tracking are thought to be inaccurate for small wingspan-to-body diameter ratios (i.e., for canards). Also, the current method of calculating body-alone loads does not include the effect of wing vortices on afterbody loads.

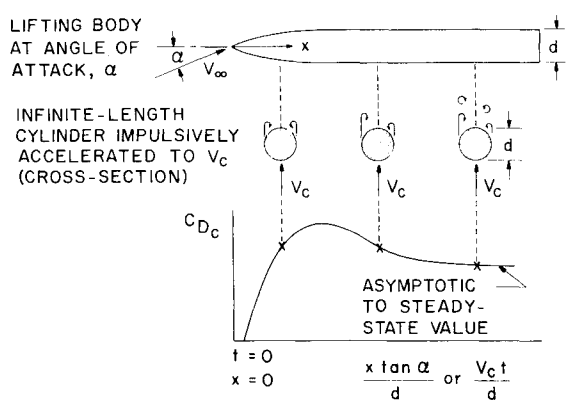

Fig. 2 Lifting body-impulsive flow analogy.

Development of the Experimental Technique

Experiments were conducted in the AEDC Aerodynamic Wind Tunnel (4T) using three models of the GBU-15 store (see Fig. 3). One model was a 1/4-scale conventional pressure model equipped with 182 static pressure orifices and four Scanivalves®. The other models were unique, segmented force models in 1/4- and 1/20-scale. The 1/4-scale model consisted of four segments, each equipped with a separate five- or six-component strain-gage balance. The 1/20-scale model consisted of three segments, each with a four-component balance. All models were tested as body-alone (B), body-wing (BW), and body-wing-canard (BWC) configurations at Mach numbers from 0.4 to 1.2 and angles of attack from -4 deg to as high as 28 deg.

Wind Tunnel

The AEDC Aerodynamic Wind Tunnel (4T) is a closed-circuit tunnel in which continuous flow can be maintained at various free-stream densities. Mach number can be varied between 0.1 and 1.3, and nozzle blocks can be installed to provide discrete Mach numbers of 1.6 and 1.96. Stagnation pressure can be varied from 300 to 3700 psfa at all Mach numbers. The test section is 4 ft^2 and 12.5 ft long with perforated, variable-porosity (0.5 to 10% open) walls. The effects of blockage and shock reflection can be reduced during testing by evacuating a portion of the airflow from the test section through the porous walls into the plenum chamber surrounding the test section. Models can be supported in the test section with a conventional sector-sting system with a pitch range of approximately from -12 to 28 deg and a roll capability of from -180 to 180 deg about the sting centerline.

Large-Scale Pressure Model

The pressure model was selected to provide a baseline configuration for validation of the segmented model concept. The 1/4-scale size chosen for the pressure model allowed a sufficiently large number of orifices to accurately determine the pressure distribution over the entire model, including the wings and canards. Pressure orifices were located along the entire body length in three rows of 34 orifices each spaced at 30-deg intervals (at $\phi = 0$, -30, and -60 deg), with an additional orifice at the nose tip. By testing at roll angles of 0, ± 90, and 180 deg and assuming model symmetry, data were obtained along longitudinal rays spaced every 30 deg around the model.

Pressure orifices were located on the $\phi = 45$-deg canard along two rows. One row of 12 orifices was located on the upper surface at a span location of 30%, and the second row, consisting of 11 orifices, was located on the lower surface, outboard of the first row at a span location of 60%. Pressure orifices were located on the $\phi = \pm 45$-deg wings along four rows of 14 orifices each at span locations of 20, 40, 60, and 80%. The rows were split between two wings, because of space limitations, with one row on the upper surface and one on the lower surface of each wing. Again, by testing at 90-deg

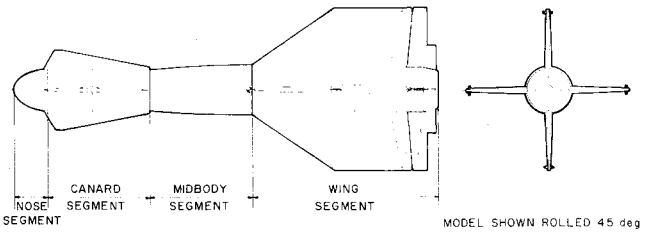

Fig. 3 Details of the GBU-15 store, with segment division locations for the 1/4-scale segmented model.

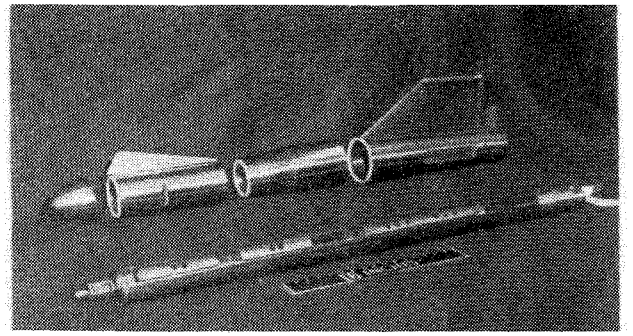

Fig. 4 1/4-scale segmented force model and sting-balance assembly.

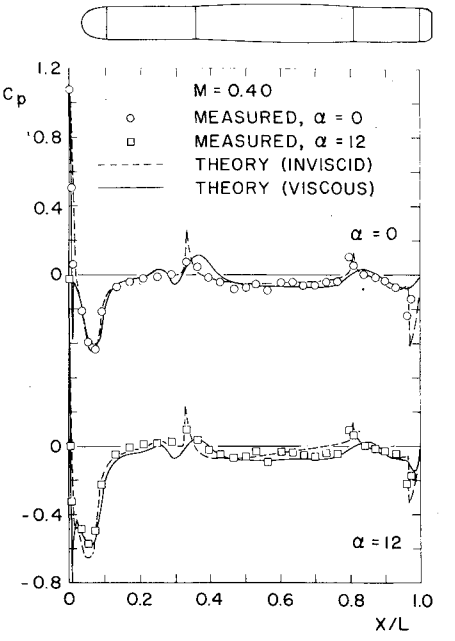

Fig. 5 Comparison of theoretical and measured pressure distributions on the 1/4-scale body-alone configuration.

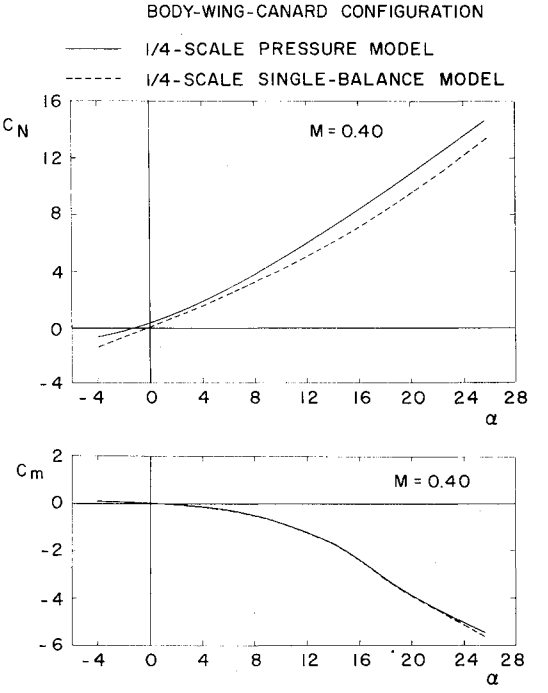

Fig. 6 Comparison of integrated 1/4-scale pressure-model data and total loads on the 1/4-scale single-balance model.

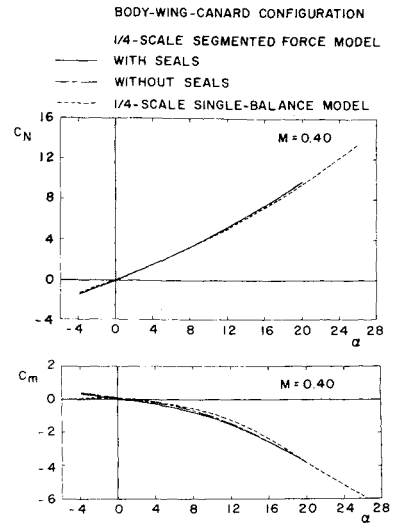

Fig. 7 Comparison of total loads on the 1/4-scale segmented force with and without seals installed between segments with total loads on the 1/4-scale single-balance model.

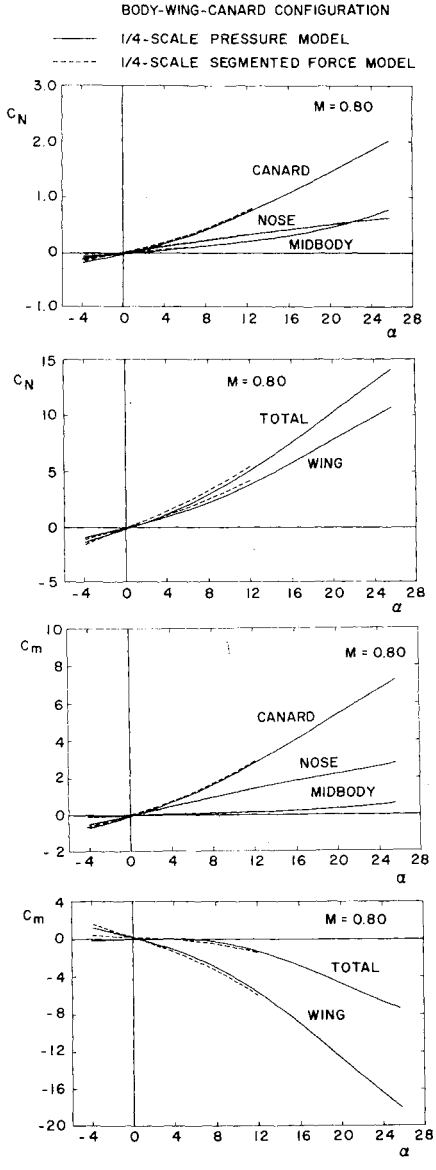

Fig. 8 Comparison of loads on the segments of the 1/4-scale segmented force model with integrated 1/4-scale pressure-model data.

roll intervals and assuming symmetry, data were obtained for each fin roll orientation.

Large-Scale Segmented Force Model

The 1/4-scale force model (Fig. 4) consisted of four segments, termed the nose, canard, midbody, and wing segments, each equipped with a separate strain-gage balance. Division points between segments are shown in Fig. 3. The canard, midbody, and wing segment balances each measured six components of force and moment. The nose balance, because of space limitations, did not measure rolling moment. The balances were mounted separately to a single sting running the entire length of the body. The sting was a unique design with a channel-shaped cross section. Balance stiffness was intentionally large, as was the sting stiffness, to minimize deflections of one model segment relative to another. The 0.01-in. gap between adjacent segments was only as wide as necessary to prevent fouling. To block flow into or out of the balance cavity in the model, seals, similar to O-rings, made from extremely flexible closed-cell plastic foam, were installed to grooves machined on both segment faces at each joint. The model was also tested without the seals installed to determine their effect on the data.

Small-Scale Segmented Force Model

The 1/20-scale force model consisted of three segments. Because a separate balance could not be mounted in the small

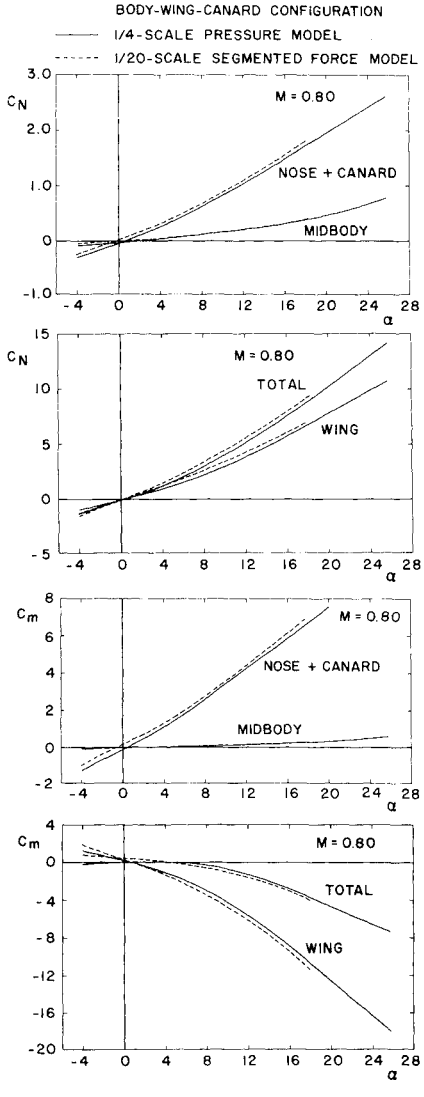

Fig. 9 Comparison of loads on the segments of the 1/20-scale segmented force model with integrated 1/4-scale pressure-model data.

nose of the model, the nose and canard regions were combined into one segment. As with the 1/4-scale force model, the segments were each equipped with a separate strain-gage balance. The balances each measured four components of force and moment; axial force and rolling moment were not measured. Again, the balances were mounted separately to a special slotted sting. Adjacent segments were separated by 0.006-in. gaps. Seals were not installed between segments both because the segment walls were much thinner than those of the 1/4-scale force model and because the 1/4-scale data indicated that the effect of the seals was minor.

A pylon-mounted version of the 1/20-scale segmented force model was tested in the carriage position on an aircraft late in FY81.

Results

Theoretical predictions of the pressure distribution for the GBU-15 body-alone case were made using both viscous and inviscid Pulliam-Steger finite-difference methodology.[11] The predictions correlated well with the measured pressure distribution (Fig. 5). Total loads on the pressure model were obtained by integrating the pressure data. A lack of pressure data on the outboard and trailing-edge regions of the canards and on the wing flaps necessitated assumptions for the pressure distribution in those areas. These assumptions caused minor discrepancies between the pressure model integrated loads and total loads measured previously on a complete force model of the same configuration.[12] The total normal-force and pitching-moment coefficients for the body-wing-canard configuration obtained by integrating pressure model data are compared with those measured on the model of Ref. 12 in Fig. 6.

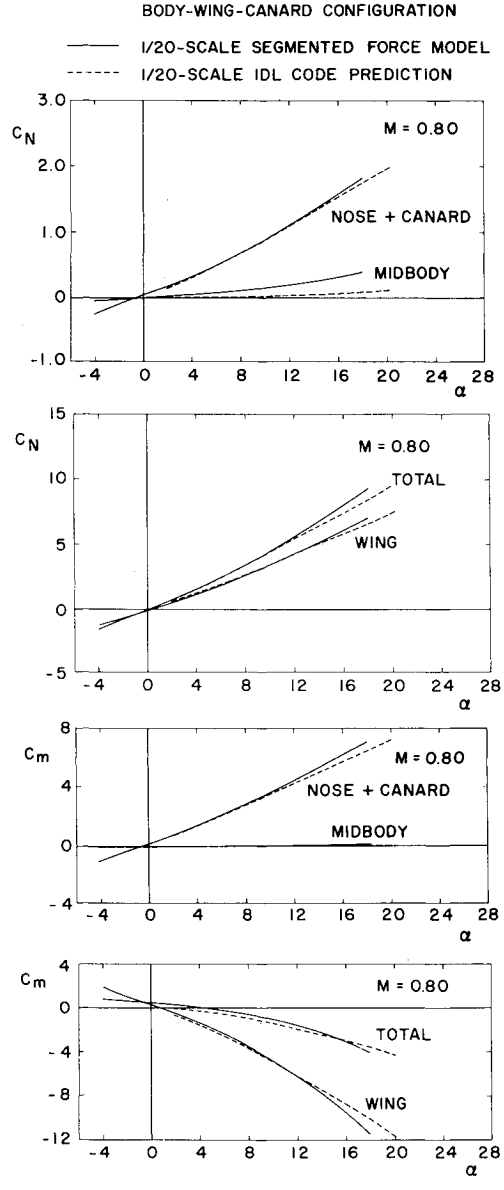

Fig. 10 Comparison of loads on the segments of the 1/20-scale segmented model with IDL code 1/20-scale predictions.

Data taken on the 1/4-scale segmented model with and without seals installed between the segments indicated that the effect of the seals was minor. Total loads on the 1/4-scale segmented model agreed very well with those on the model of Ref. 12 (see Fig. 7). Loads measured on the individual segments of the 1/4-scale segmented model compared well with integrated pressure model data (Fig. 8), as did loads meausured on the segments of the 1/20-scale segmented model (Fig. 9). Comparing Figs. 8 and 9 indicates that total normal-force and pitching-moment coefficients on the 1/4- and 1/20-scale segmented models were nearly identical, demonstrating that scale effects were minor.

Predictions made using the IDL code for the body-wing-canard case are compared with 1/20-scale segmented model data in Fig. 10. Altogether, the predictions agree well with the experimental data. The code underpredicts the loads on the midbody segment because of its inability to model the increasing diameter of the midbody. The discrepancies in normal-force and pitching-moment coefficients on the wing segment at high angles of attack are probably partially attributable to an overprediction of body vortex strength.

Conclusions

A semiempirical code was developed which provides quick and reasonably accurate predictions of aerodynamic loads and their distribution on complex store configurations for a wide range of flight conditions in the free-stream. The code has been extended to provide the capability of making predictions in an interference flow-field. Areas where further methodology refinements may be desirable have been identified.

An experimental technique was developed to measure load distributions on stores in a wind tunnel by using a segmented model with separate balances for each segment. The validity of the technique was established by comparing the data from a large-scale four-segment model with data from a large-scale pressure model and was extended to a smaller scale using a three-segment model of the same configuration. A small-scale segmented model was recently tested in the carriage position on an aircraft, providing data for validation of the interference flow-field distributed loads prediction technique.

Acknowledgments

The research reported herein was performed by the Arnold Engineering Development Center, Air Force Systems Command. Work and analysis for this research were done by personnel of Calspan Field Services, Inc., AEDC Division, operating contractor of the aerodynamic testing facilities at AEDC, and of the Air Force Armament Laboratory. Further reproduction is authorized to satisfy the needs of the U.S. Government.

References

[1]Koshar, M.M. et al., "Computer Aided Missile Synthesis (CAMS)," Martin Marietta Corporation, Orlando, Fla., OR 12,034, June 1972.

[2]Kellock, R.E. and Miller, P.H., "Aerodynamic Characteristics of Basic Nose-Cylinder Bodies for Large Ranges of Angle of Attack," Department of Mechanical, Aerospace and Industrial Engineering, Louisiana State University, Baton Rouge, 1971.

[3]Jorgensen, L.H., "Prediction of Static Aerodynamic Characteristics for Slender Bodies Alone and With Lifting Surfaces to Very High Angles of Attack," NASA TR R-474, Sept. 1977.

[4]Fidler, J.E. and Bateman, M.C., "Aerodynamic Methodology (Isolated Fins and Bodies)," Martin Marietta Corporation, Orlando, Fla., OR 12,399, March 1973.

[5]Thomson, K.D., "The Estimation of Viscous Normal Force, Pitching Moment, Side Force and Yawing Moment on Bodies of Revolution at Incidences up to 90°," Weapons Research Establishment, Salisbury, South Australia, WRE-Report-782 (WR&D), Oct. 1972.

[6]Sarpkaya, T., "Impulsive and Accelerated Flow About Cylinders," NASA TMX-57779, 1966.

[7]Nielsen, J.N., Hemsch, M.J., and Smith, C.A., "A Preliminary Method for Calculating the Aerodynamic Characteristics of Cruciform Missiles to High Angles of Attack Including the Effects of Roll Angle and Control Deflections," Office of Naval Research, ONR-CR-215-226-4F, Nov. 1977.

[8]Pitts, W.C., Nielsen, J.N., and Kaattari, G.E., "Lift and Center of Pressure of Wing-Body-Tail Combinations at Subsonic, Transonic and Supersonic Speeds," NACA Report 1307, 1957.

[9]Koshar, M.M. et al., "Computer Aided Missile Synthesis (CAMS)," Martin Marietta Corporation, Orlando, Fla., OR 15,185, Aug. 1978.

[10]Finck, R.D. et al., "USAF Stability and Control DATCOM," McDonnell Douglas Corporation, Douglas Aircraft Division, Oct. 1960; revised April 1978.

[11]Pulliam, T.H. and Steger, J.L., "Implicit Finite-Difference Simulations of Three-Dimensional Compressible Flow," *AIAA Journal*, Vol. 18, Feb. 1980, pp. 159-167.

[12]Kaupp, H. Jr. and Carman, J.B. Jr., "Aerodynamic and Aircraft Separation Characteristics of the Electro-Optical Guided Bomb II (EOGB II)," Arnold Engineering Development Center, Arnold AFS, Tenn., AEDC-TR-75-66 (AD-B0044722), June 1975.